Studia Geotechnica et Mechanica, Vol. XXXV, No. 1, 2013 DOI: 10.2478/sgem-2013-0017

QUICK SANDS EFFECT ON DESERT LANDS – EXAMPLE OF FILTRATION STABILITY LOSS

MICHAŁ STRZELECKI

KGHM CUPRUM Ltd. Research and Development Centre,
ul. Gen. Wł. Sikorskiego 2–8, 53-659 Wrocław, Poland. E-mail: mstrzelecki@cuprum.wroc.pl

Abstract: The aim of the study was to analyze the loss of filtration stability of fine desert sands due to the air flow caused by temperature difference. The loss of stability induces the effect of so called "quick sands". Therefore, the calculations of air filtration through the loose sand medium in dry desert climate are presented. FlexPDE v.6. software was used for numerical calculation based on FEM.

1. INTRODUCTION

Based on state-of-the-art [8], quick sand is the so-called "non-Newtonian fluid" – mixture of silica grains and water. In normal sands grains are closely packed, which is a bit as if the soil were compressed. For example, on the beach, wind and treading people press the grains, which in result gives the stable soil. However, in specific conditions the sand may be far less compact. For example, in dunes where grains poured and raised by wind are more open-grained. In such places quick sands can be easily found. When it rains heavily there, sand grains are much more moved away from each other, and the space between them is filled by water. The trappy suspension – the kind of mud, called quick sands – arises.

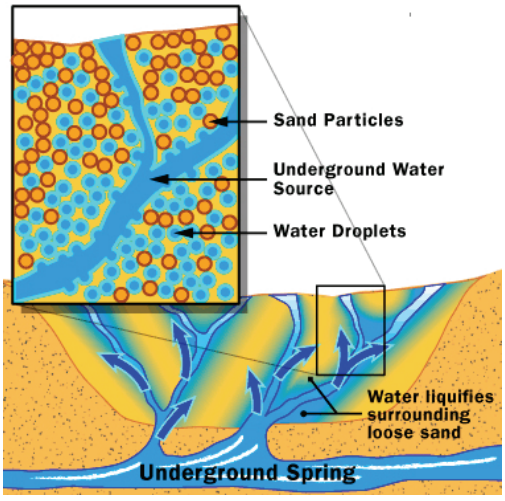

Fig. 1. Liquefaction effect on sandy areas

It is an effect occurring only in sandy areas and under specific conditions. Most often the reason is the situation when water, which locally cannot find the escape, saturates the area of loose sand [9]. The medium in form of suspension, which loses its primary properties, is formed then. There are several cases where the filtration stability may be lost:

a) ground water – flowing under the pressure towards the surface, compensates the gravity and the sand grains remain loosely suspended in the flowing water (Fig. 1).

b) earthquakes – stresses arising during earth tremors result in an increase of underground water pressure, which may cause the liquefaction.

The effect of quick sands may occur at almost any site where water is present, however, there are certain places where it is more common. It may be a river bank, beach, lake shore, a site close to underground sources or swamp.

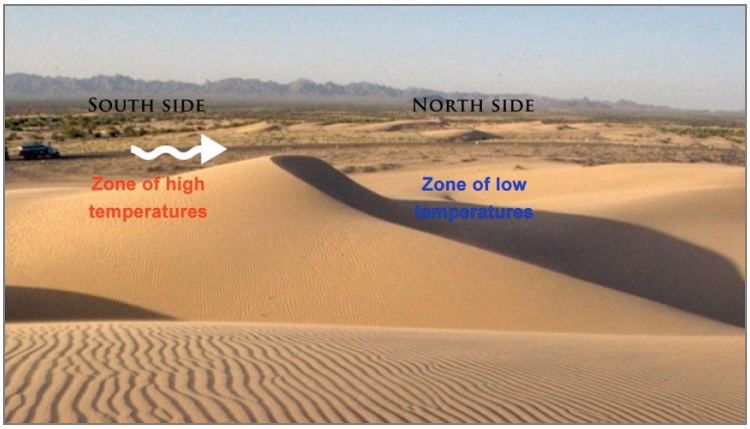

Fig. 2. Example of desert dunes location

Not negating the above interpretation of the effect reasons, the paper presents a different mechanism of the process. Now, in desert areas from February to the end of November, there is no precipitation at all, but the quick sand effect is encountered. Over big desert areas dunes are located along east–west line, because the winds mostly blow from south towards north. South slopes of dunes are inclined at a very small angle and on their surface the sand temperature is very high during the day. North slopes are steep and form the shadow zone, where the sand temperature is much lower than on the south side (Fig. 2). Animals seeking shadow and often people trying to hide there from burning solar radiation are taken aback by quick sands. The air and heat flow through loose and porous medium using the thermo-filtration equations for two-phase medium, derived by the author in separate publication, were calculated there. Calculations of vector field of air flow velocity, pressure distribution, scalar area of temperature were made applying the FEM and using Flex PDE v.6 [7] software.

2. MATHEMATICAL MODEL OF FILTRATION FLOW OF GAS

A mathematical model of filtration flow of gas and heat through the porous medium was defined under the following initial assumptions:

- the medium is an undeformable two-phase one and is composed of undeformable frame and compressible, adhesive fluid filling the medium pores,
- the medium is homogenous and isotropic,
- dynamic effects are not taken into consideration, the process of flow is regarded as quasi-static,
- the porosity of the medium is defined by, invariable during the process of flow, f – coefficient of cubical porosity,
- the process of gas compression is defined by the equation of real gases state,
- the function of dissipation, after Strzelecki et al. [5], is a square form dependent on velocity of filtration flow, which may be expressed as follows

$$2W_d = \int_{\Omega} b v_i^2 d\Omega \tag{1}$$

where $\vec{v}$ is the vector of filtration velocity, and b is a parameter describing averaging coefficient of resistance of adhesive environment.

2.1. EQUATION OF FLOW CONTINUITY

It is assumed that Ω is a space filled by a two-phase medium frame and the fluid filling its pores. S defines the area confining the spatial element Ω, $\vec{n}$ is a unit vector normal to S area, directed outside Ω element.

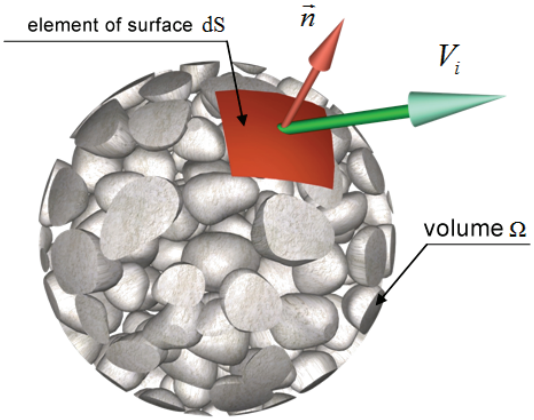

Fig. 3. Representative volume element (after Bartlewska [1])

If ρ_l means specific density of gas, it is possible to define ρ – the density of gas related to the total volume of area Ω. Determining the volume porosity as f it is possible to calculate density $\rho = f\rho_l$.

An equation of continuity of gas flow through porous environment has the form

$$\int_S \rho v_i n_i dS + \int_\Omega \frac{\partial \rho}{\partial t} d\Omega = 0 . \tag{2}$$

After taking into consideration the Gauss–Ostrogradski theorem, the above equation can be as follows

$$\int_\Omega \operatorname{div}(\rho v) d\Omega + \int_\Omega \frac{\partial \rho}{\partial t} d\Omega = 0 \tag{3}$$

which makes for the local relation

$$\operatorname{div}(\rho v) = \frac{\partial \rho}{\partial t} . \tag{4}$$

2.2. EQUATION OF MOMENTUM CONSERVATION

The equation of momentum conservation for i-component of force as a form of d'Alambert formula

$$\int_S \sigma n_i dS - \int_\Omega b v_i d\Omega + \int_\Omega \rho X_i d\Omega = \int_\Omega \frac{\partial v_i}{\partial t} d\Omega \tag{5}$$

where

$$\sigma = -p f \tag{6}$$

means the porous tension of gas.

The above equations lead to the local equation of gas movement

$$\sigma_{,i} - b v_i + \rho X_i = \rho \frac{\partial v_i}{\partial t} . \tag{7}$$

This equation in quasi-static case, according to Strzelecki et al. [6], leads to the classic Darcy equation

$$v_i = -k \frac{\partial H}{\partial x_i} \tag{8}$$

where $k = \rho g / b$ and $H = \dfrac{p}{\rho g} + x_i \delta_{i3}$.

2.3. CONSTITUTIVE EQUATIONS AND ENTROPY EQUATION

Constitutive equations and entropy equation may be derived from thermodynamic law for irreversible processes. The methodology presented by Nowacki [3] to define the thermo-elasticity was used in the study.

Coming from the first thermodynamic law

$$\dot{L} + \dot{Q} = \frac{\partial}{\partial t}(W + K), \tag{9}$$

for the case considered the following equation

$$\int_S \rho v_i n_i dS + \int_\Omega \rho X_i v_i d\Omega - \int_\Omega b v_i^2 d\Omega - \int_\Omega q_i d\Omega = \int_\Omega \left(\frac{\partial w}{\partial t} + \rho v_i \frac{\partial v_i}{\partial t} \right) \tag{10}$$

is obtained.

After taking into consideration the equations of momentum conservation, the equation defining the change of inner energy of gas is obtained

$$\dot{w} = \sigma \dot{\theta} - q_{i,i}. \tag{11}$$

In order to define the limitation of directions of the system status changes, the second thermodynamic law introduces the inequality stating that the change of inner entropy of system is always positive or equal zero, known as the Clausius–Duhem inequality. According to De Groot, Mazur [2] the function of specific entropy s, measured for the unit of volume Ω, is introduced

$$S = \int_\Omega s d\Omega. \tag{12}$$

The specific entropy is defined as

$$s = \frac{dq}{T} \tag{13}$$

where T is the absolute temperature of gas.

Then using the definition of free energy of Helmholtz for adiabatic processes, after developing this function into Taylor series, the physical relation is obtained

$$\sigma = a_3 \theta + a_1 T \tag{14}$$

as well as equation describing the entropy function

$$-s = a_1 \theta + a_2 T. \tag{15}$$

2.4. SYSTEM OF EQUATIONS FOR THERMO FILTRATION

The above equations allow us to create the system of equations of thermo-filtration of gas through undeformable porous medium having the following form

$$\begin{aligned} \operatorname{div}(\operatorname{grad}(\sigma)) &= p_3\dot{\sigma} + p_4\dot{T}, \\ \operatorname{div}(\operatorname{grad}(T)) &= p_1\dot{\sigma} + p_2\dot{T}, \end{aligned} \tag{16}$$

where

$$p_1 = \frac{\alpha_T RT}{\lambda_T}, \quad p_2 = \frac{\rho c_v}{\lambda_T},$$
$$p_3 = \frac{\rho g f}{Rk}, \quad p_4 = \frac{\rho g f \alpha_T}{k},$$

α_T means volumetric expansion of gas, R compressibility of gas, λ_T thermal conductivity of gas, c_v specific heat at constant volume.

2.5. FILTRATION POTENTIAL

Defining the condition of filtration stability requires determination of the potential of filtration flow area. The components of mass forces of filtration are expressed as follows

$$p_{si} = \rho g \frac{v_i}{k}. \tag{17}$$

Knowing that the components of speed vector are expressed through the hydraulic gradient, vector of forces affecting the ground framework, taking into consideration the gravitation force, is expressed by the formula

$$\vec{S} = -\rho g * \operatorname{grad}(H) - \vec{\Delta}^* \tag{18}$$

where $\vec{\Delta}^*$ defines the gravity forces of framework per volume unit.

Since the vector field of filtration forces, like gravity field, is a potential field, it can be stated that the sum of those fields impact is also a potential field. If we assume that $\Re$ is a potential of this resultant field of forces, the following relation must be performed

$$\vec{S} = \operatorname{grad}(\Re). \tag{19}$$

Finally using the formulas (18) and (19) the following form of filtration potential function $\Re$ is obtained

$$\Re = -(\rho g H + \vec{\Delta}^* \delta_{i3} x_i). \tag{20}$$

In [6] it was shown that when $\frac{\partial \Re}{\partial x_3} > 0$ the loss of filtration stability and soil liquefaction takes place.

3. NUMERICAL MODEL OF AIR THERMO-FILTRATION

The issue of filtration flow of air through porous environment, which should imitate air filtration through desert dunes as a result of laps rate is presented in 2D in Fig. 4, where one slope of dune is sun-lit and has high temperature, while the other is in the shadow zone and its temperature is much lower. Figure 4 presents also geometry area and the grid of finite elements generated by FlexPDE v.6 software.

Effective parameters for calculating the thermo-filtration model are listed in Table 1.

Table 1

Effective parameters of thermo-filtration model of air

f	c_v	R	λ_T	k
	$\frac{\text{J}}{\text{kg K}}$	$\frac{1}{\text{Pa}}$	$\frac{\text{W}}{\text{m K}}$	$\frac{\text{m}}{\text{s}}$
0.4	1000.8	1e-5	0.025	1e-4

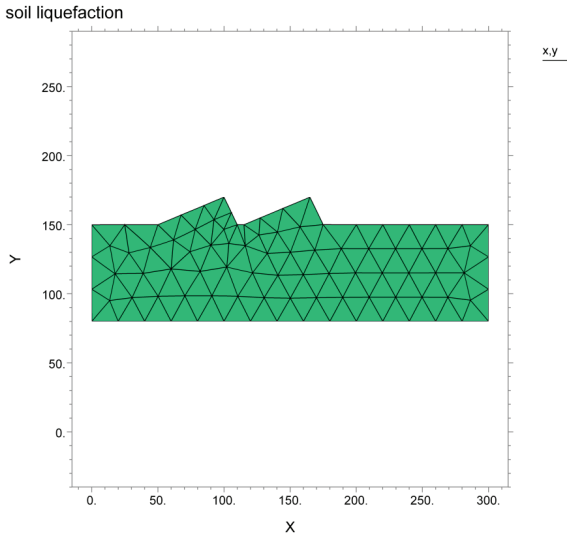

Fig. 4. Shape of calculation area and grid of finite elements

Air density changes with temperature. The formula for calculating this parameter according to [4] is

$$\rho = -\frac{\sigma}{R_p f T} \tag{21}$$

where R_p means individual Clapeyron constant for air.

The process of air filtration through sand was observed under periodical temperature changes both on sunny (T0) and shadow (T1) side. Accordingly, the functions of temperature changes with time were adopted in the following form

$$\begin{aligned} T0 &= 303 + \left|\sin\left(\frac{\pi * t}{86400}\right)\right| * 70, \\ T1 &= 293 + \left|\sin\left(\frac{\pi * t}{86400}\right)\right| * 20. \end{aligned} \tag{22}$$

Those functions assume that maximum sand temperature on sunny side is 100 °C, and the lowest temperature drops down to 30 °C. This temperature range seems to be possible, in spite of the fact that at night the temperature in the desert falls to 10 °C. However, nights are short and the sand is not able to cool to the air temperature. Then it was assumed that temperature T1 in the shadow area changes from 20 °C to 40 °C.

Variability of temperatures during 1 month is presented in Fig. 5.

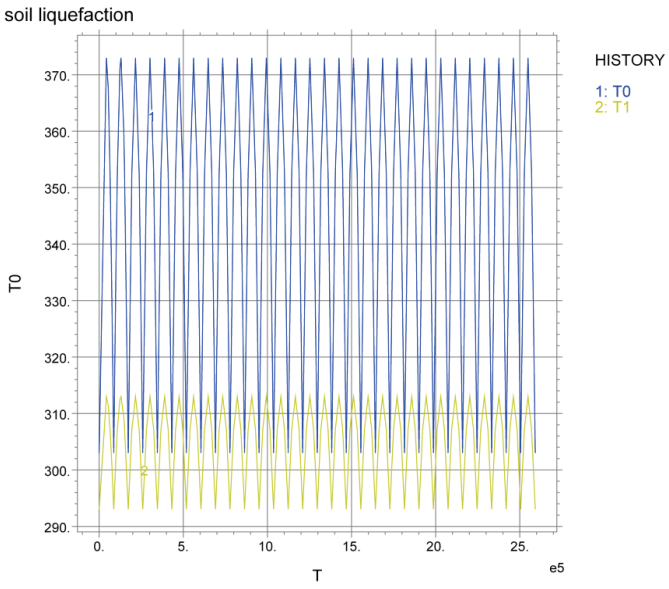

Fig. 5. Variability of temperatures during 1 month

It was also assumed that initial value of the sand temperature is 30 °C.

4. RESULTS OF NUMERICAL CALCULATIONS

Calculations resulted in, changing with time, scalar fields of hydraulic head and sand temperature, vector fields of filtration speed and heat flowing through the soil, charts of filtration stability potential as well as chart of variability of air density flowing through the sand.

Variability of temperature field during the day cycle is presented in Fig. 6. Figure 6(a) shows the temperature distribution at the lowest ambient temperature (middle of the night). Figure 6(b) illustrates the temperature distribution after 6 hours, Fig. 6(c) at maximum ambient temperature after 12 hours, and finally, Fig. 6(d) after 18 hours.

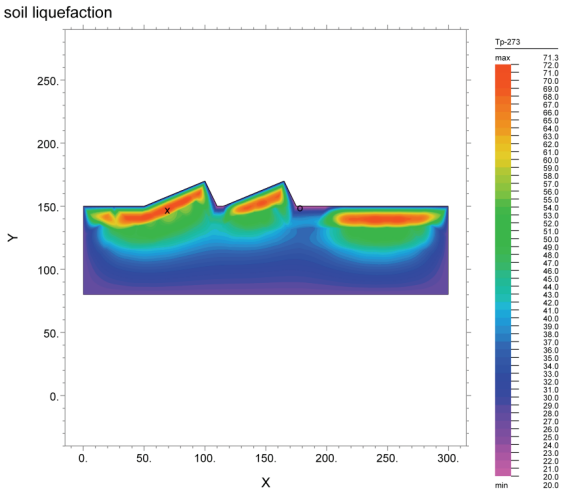

a)

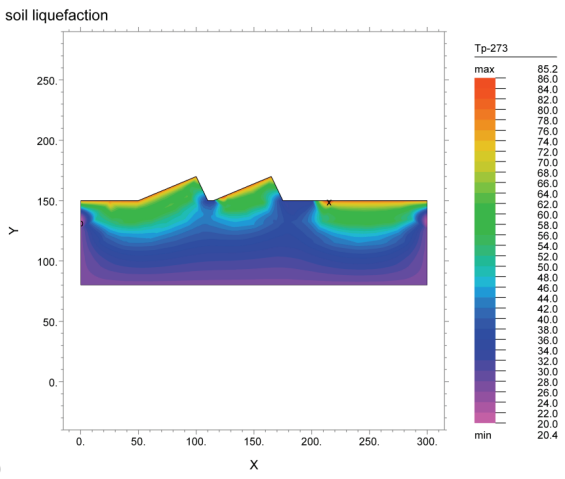

b)

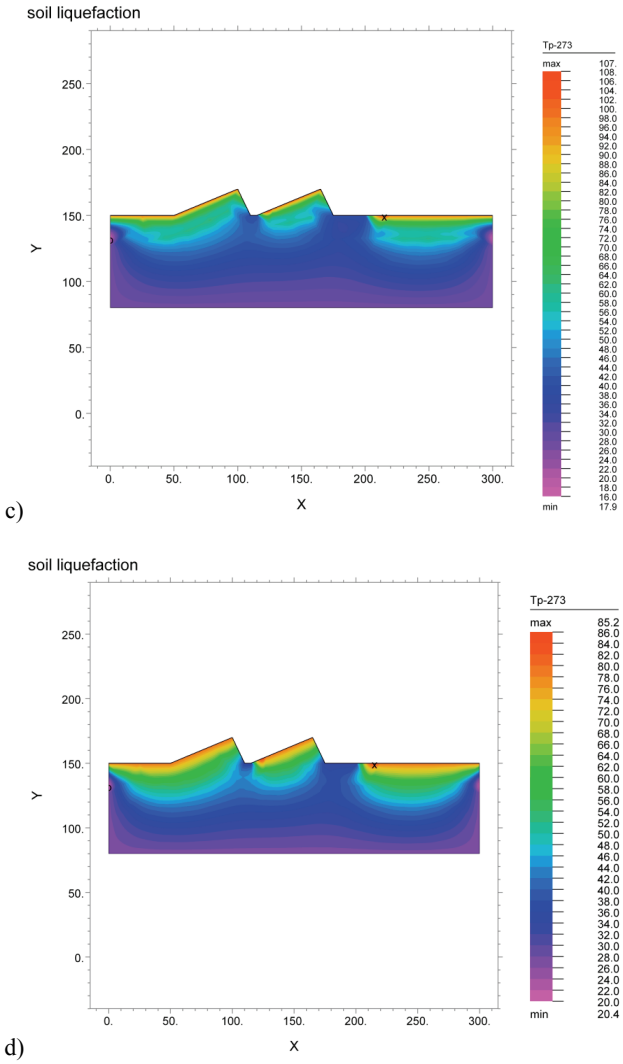

Fig. 6. Distribution of temperature in sand in the vicinity of dunes during 24 hours: (a) night, (b) morning, (c) temperature during the day, (d) evening

In Figure 7, the vector field of air velocity during its flow through dunes for maximum and minimum ambient temperature is presented.

As can be seen during the cooling period the outflow of heated air to the atmosphere takes place and speed vectors are directed towards the edge of area. The other way around, when the ambient temperature is the highest, air flows from the heated zones to the ones with lower temperature. Close to the sites with low temperature, the filtration speed vector has the vertical component oriented upwards.

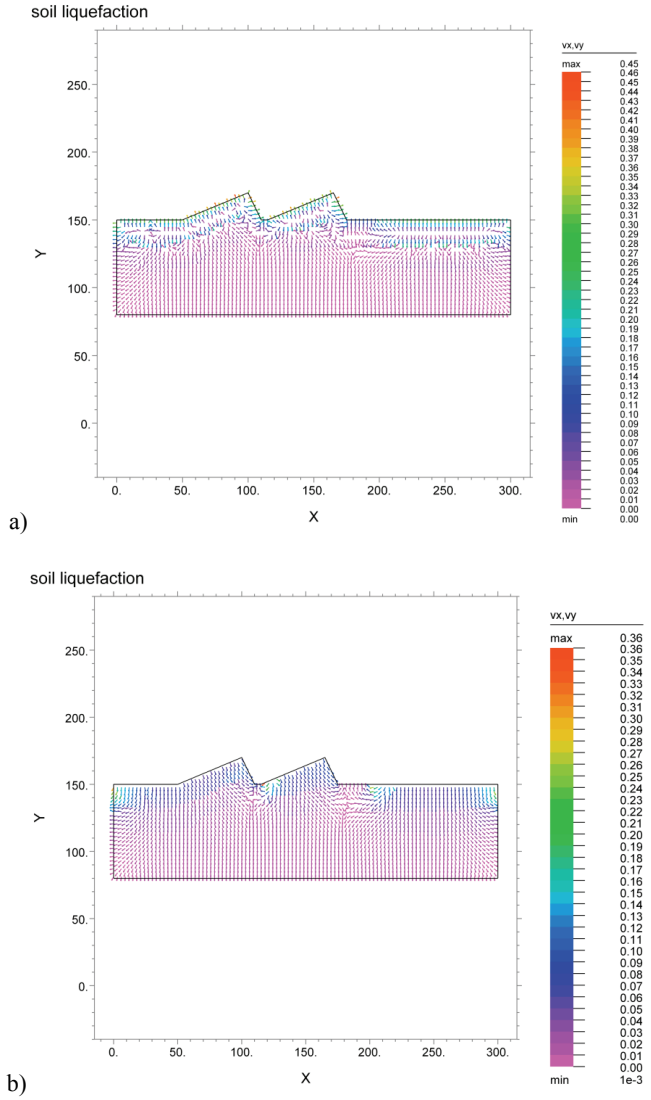

Fig. 7. Vector field of air flow velocity;
(a) for minimum ambient temperature, (b) for maximum ambient temperature

Essential part of calculations is evaluation of filtration stability of dunes under, variable in time, air flow through the sand. Figure 8 presents the charts derivate of filtration potential $\frac{\partial \Re}{\partial y} > 0$, depending on ambient temperature for the lowest temperature after 6, 12 and 18 hours, enlarged for the part of area under investigation.

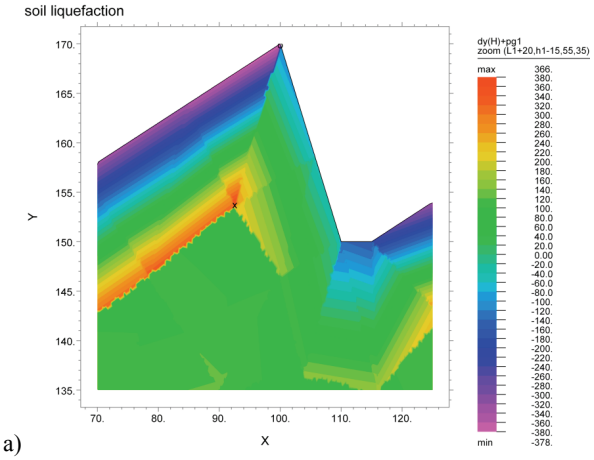
soil liquefaction
dy(H)+pg1
zoom (L1+20,h1-15,55,35)
max
366.
380.
360.
340.
320.
300.
280.
260.
240.
220.
200.
180.
160.
140.
120.
100.
80.0
60.0
40.0
20.0
0.00
-20.0
-40.0
-60.0
-80.0
-100.
-120.
-140.
-160.
-180.
-200.
-220.
-240.
-260.
-280.
-300.
-320.
-340.
-360.
-380.
min
-378.
Y
170.
165.
160.
155.
150.
145.
140.
135.
70.
80.
90.
100.
110.
120.
X

a)

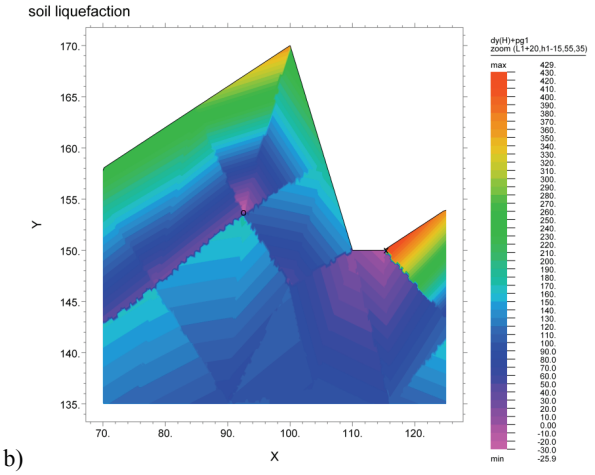
soil liquefaction
dy(H)+pg1
zoom (L1+20,h1-15,55,35)
max
429.
430.
420.
410.
400.
390.
380.
370.
360.
350.
340.
330.
320.
310.
300.
290.
280.
270.
260.
250.
240.
230.
220.
210.
200.
190.
180.
170.
160.
150.
140.
130.
120.
110.
100.
90.0
80.0
70.0
60.0
50.0
40.0
30.0
20.0
10.0
0.00
-10.0
-20.0
-30.0
min
-25.9
Y
170.
165.
160.
155.
150.
145.
140.
135.
70.
80.
90.
100.
110.
120.
X

b)

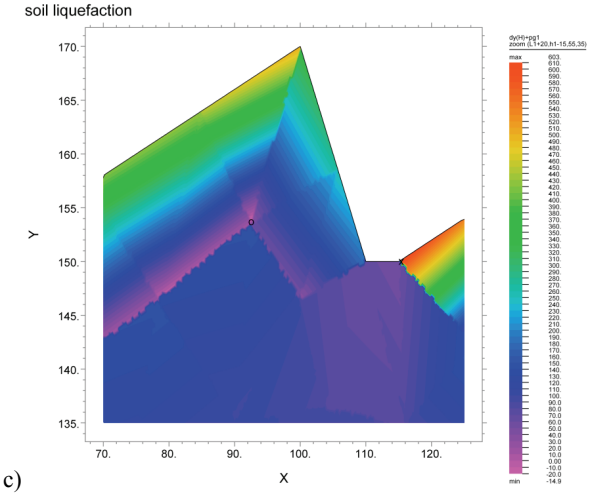
soil liquefaction
dy(H)+pg1
zoom (L1+20,h1-15,55,35)
max
603.
610.
600.
590.
580.
570.
560.
550.
540.
530.
520.
510.
500.
490.
480.
470.
460.
450.
440.
430.
420.
410.
400.
390.
380.
370.
360.
350.
340.
330.
320.
310.
300.
290.
280.
270.
260.
250.
240.
230.
220.
210.
200.
190.
180.
170.
160.
150.
140.
130.
120.
110.
100.
90.0
80.0
70.0
60.0
50.0
40.0
30.0
20.0
10.0
0.00
-10.0
-20.0
min
-14.9
Y
170.
165.
160.
155.
150.
145.
140.
135.
70.
80.
90.
100.
110.
120.
X

c)

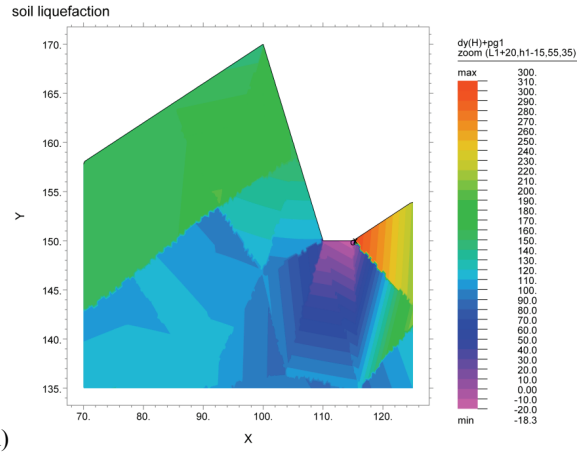

Fig. 8. Magnitude of filtration stability potential for 4 time moments

As can be seen from the charts, the derivative of filtration potential $\frac{\partial \Re}{\partial y}$ changes the sign practically for all ambient temperatures. During the period of the lowest temperature, the vectors of filtration, practically on the whole, are oriented upwards, so no wonder that the potential changes the sign, which testifies to the soil liquefaction. Along with the increase of temperature, the liquefaction occurs only in the area of shady soil. The biggest area of soil liquefaction occurs after 18 hours – in the evening. It seems that the results well project the real course of soil liquefaction and rightly explain the reason of quick sands formation.

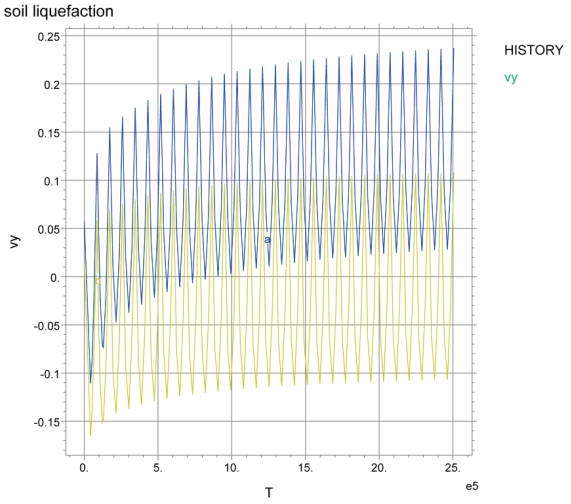

Fig. 9. Variability of vertical component of speed

Variability within the 24 hours cycle of the process of air flow through the sand does not take into consideration the evolution of processes lasting longer, for example, 1 month. Therefore, a chart of varisability of the speed vector vertical component for 30 days was made. Results for two selected points are presented in Fig. 9.

This chart shows that with time, under repeated climate conditions, during one day (24 hours) the magnitude of vertical components increases. This means that the risk of quick sand formation rises with time during the heat wave periods.

5. SUMMARY

The numerical calculations presented here confirm the author's assumptions that the cause of quick sands occurrence is the air filtration through the pores of loose medium being a result of temperature gradient. Processes of air flow are of the cyclic character. During nights, when the air temperature in summer falls to 10 °C, the air outflow from the soil takes place, and therefore the upper part of sand looses up. It has the vital impact on the bulk density of sand, which in the case of loose sand is very small. It may additionally affect the ability of desert soils to decline their filtration stability. During the day hours quick sands form in shady areas, where the ambient temperature is lower than in sunny spaces. This may be surprising for people travelling across the desert. It is especially dangerous for the desert animals, which cannot get along with that effect.

As was shown on the chart of Fig. 9 the value of the vertical component of flow rate vector increases with time. Thus, the desert sands after long period of heat wave are much more susceptible for generating quick sands.

REFERENCES

[1] BARTLEWSKA M., *Defining parameters of effective rheological models of cohesive soils*, doctoral dissertation, (in Polish), Wrocław University of Technology, Faculty of Geo-engineering, Mining and Geology, Wrocław 2009.
[2] DE GROOT S.R., MAZUR P., *Non equilibrium Thermodynamics*, Dover Publ., 1962.
[3] NOWACKI W., *Theory of elasticity*, (in Polish), PWN, 1970.
[4] SALEJDA W., POPRAWSKI R., JACAK L., MISIEWICZ J., *Thermodynamics*, (in Polish), Wrocław University of Technology, Faculty of Physics, 2001.
[5] STRZELECKI T., BAUER J., AURIAULT J.L., *Constitutive equation of a gas-filled two-phase medium*, 1993, Transport in porous media 10, 197–202.
[6] STRZELECKI T., KOSTECKI S., ŻAK S., *Modeling of flows through porous media*, (in Polish), DWE, 2008.
[7] www.pdesolutions.com
[8] www.focus.pl
[9] http://science.howstuffworks.com/environmental/earth/geology/quicksand1.htm